



Supplementary Information for

Adaptive differentiation and rapid evolution of a soil bacterium along a climate gradient

Alexander B. Chase, Claudia Weihe, and Jennifer B. H. Martiny

AB Chase
Email: abchase@uci.edu

This PDF file includes:

Figures S1 to S9
SI References

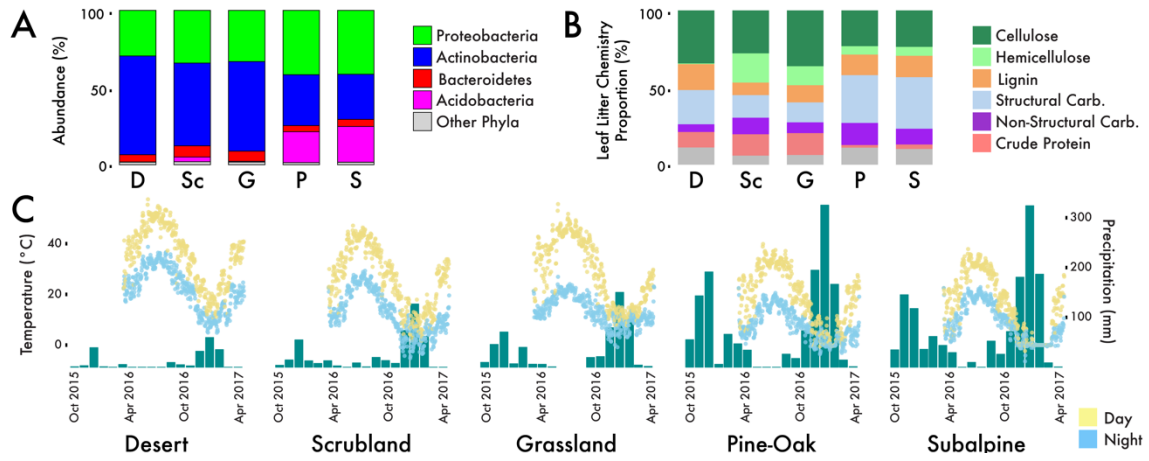


Fig. S1. Biotic and abiotic characteristics of the five sites along the elevation gradient. **A)** Relative abundance of four most abundant phyla in the survey leaf litter bacterial communities; taxa averaged across replicate plots. **B)** Mean leaf litter chemistry of non-ash dry weight from the dry season and wet season in 2015 (data from (1)). **C)** Surface soil temperature colored by day- or night-time measurement and total precipitation during the duration of the field experiment.

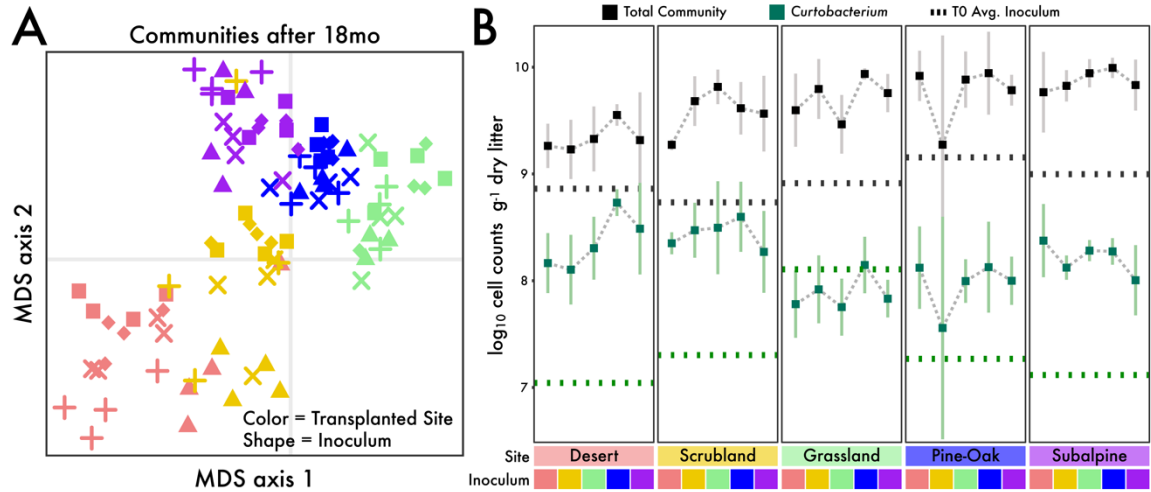


Fig. S2. Demographic shifts from the transplant experiment. **A)** Bacterial community composition after 18 months of transplant. Multidimensional scaling (MDS) plot depicting the difference in microbial communities. Symbols represent a metagenomic sample colored by site with shapes reflecting the initial litter inoculum. **B)** Absolute abundance of *Curtobacterium* and the total bacterial community. Dashed lines show abundances of initial inoculum at time point 0 at each site. Points show abundances of community and *Curtobacterium* after 18 months transplanted to each site. Error bars reflect standard deviations across 4 replicate plots.

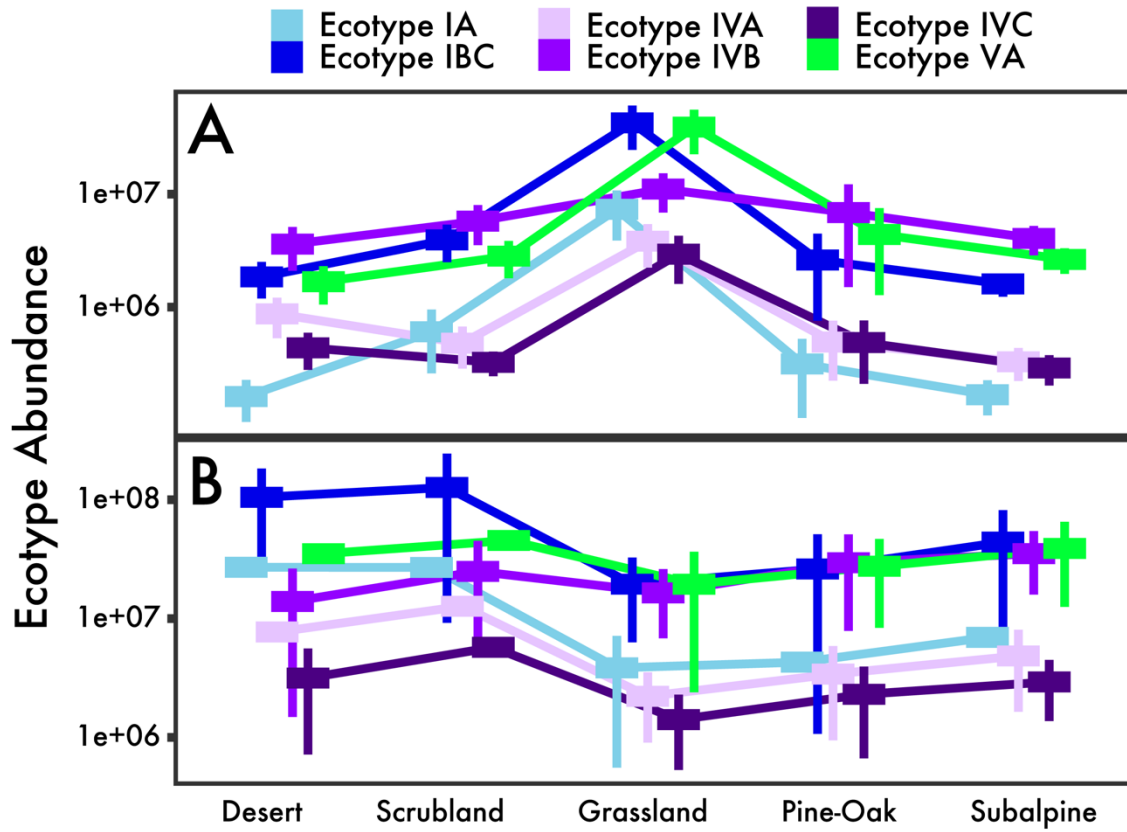


Fig. S3. Absolute abundances (by cell counts) of the top six abundant *Curtobacterium* ecotypes (± 1 SD) by site **A)** for the initial inoculum from survey samples and **B)** after an 18-month transplant experiment.

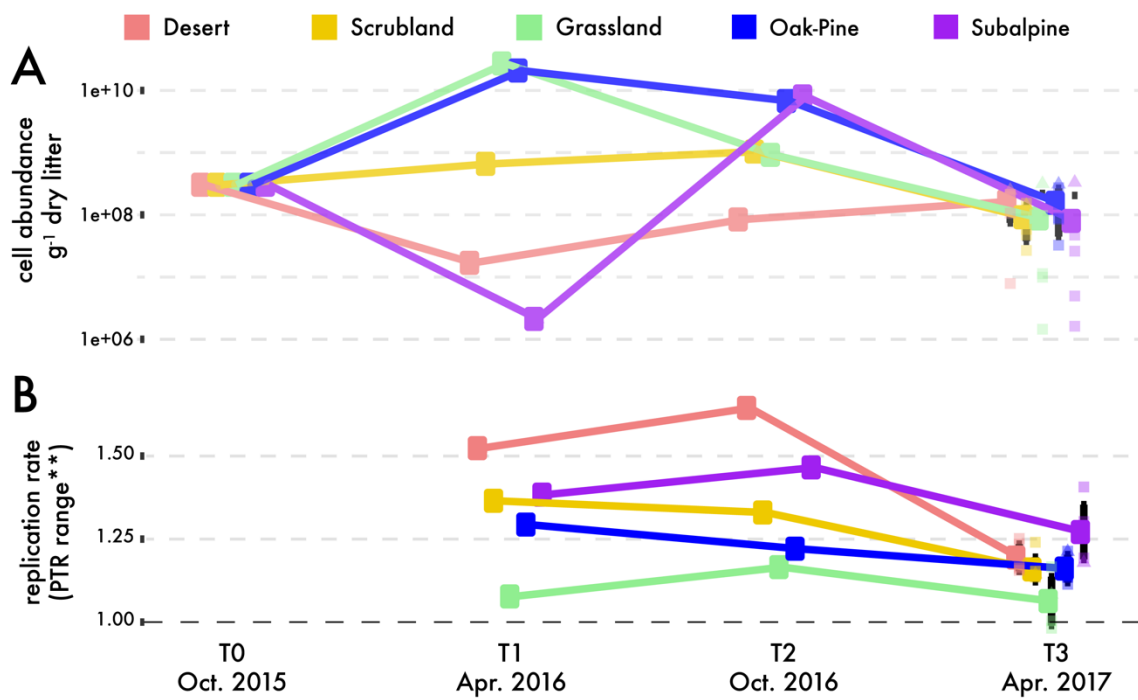


Fig. S4. Estimates of *Curtobacterium* strain MMLR14002 populations across sites and time points. **A)** Estimated number of cells based on normalization to flow cytometry cell counts. **B)** Relative replication rate estimates based on differential coverage of the ancestral genome from metagenomic reads. ******No growth (PTR (peak to trough ratio) = 1.0) denoted in black.

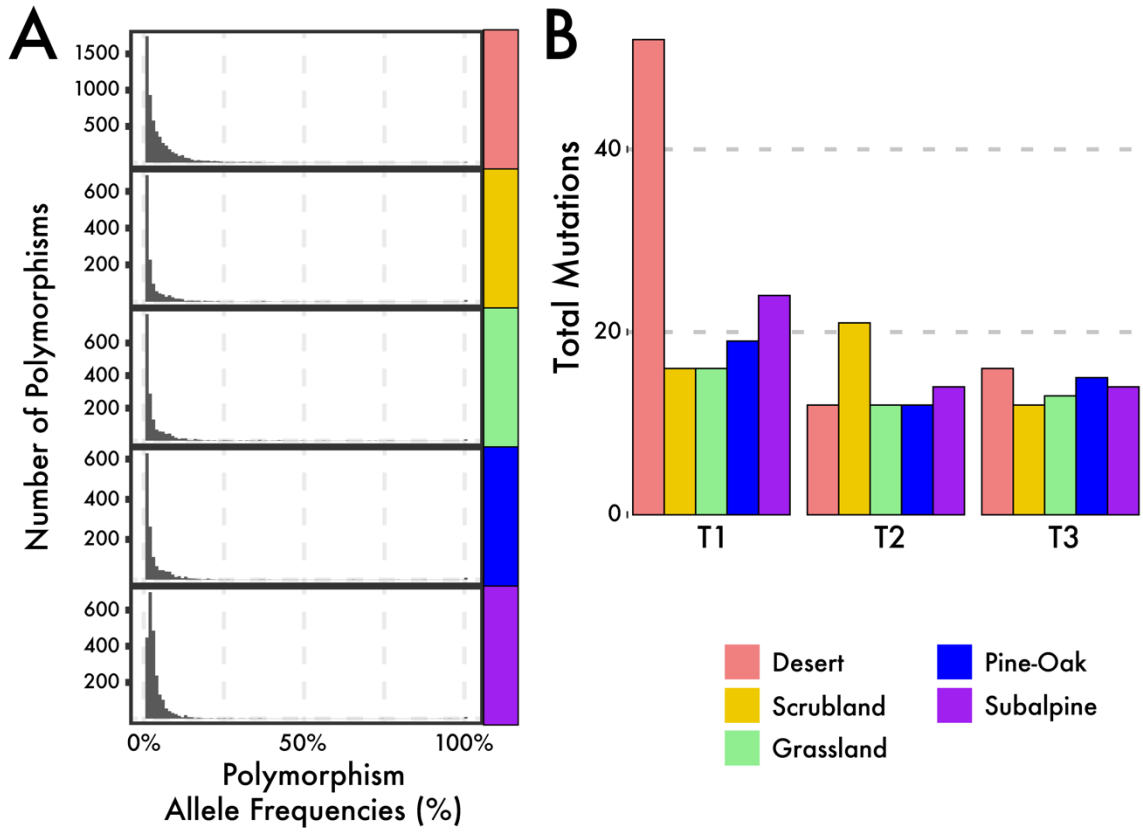


Fig. S5. Population genetic diversity of *Curtobacterium* IB/C strain MMLR14002. **A)** The number of polymorphisms observed across all sites by allele frequencies (%). **B)** Number of high-quality variants across sites and time points.

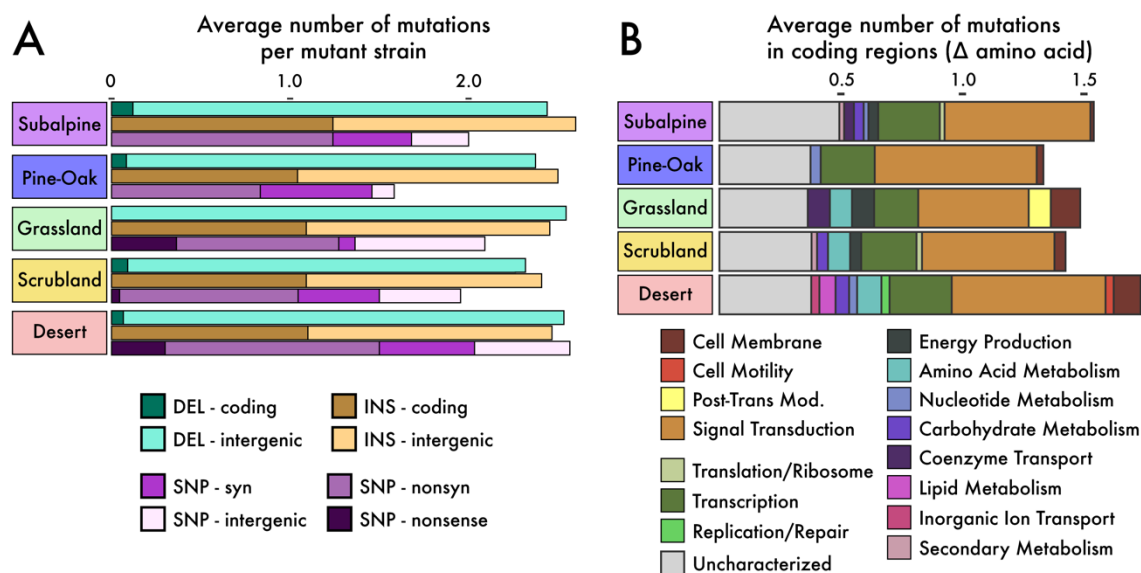


Fig. S6. Summary of mutations across sites. **A)** Average number of mutations in each mutant strain by mutation type (i.e., SNP or indel). Each mutation type is further broken down into sub-categories for coding or intergenic regions. **B)** Average number of mutations per mutant strain resulting in changes to an amino acid sequence of annotated genes. Genes were categorized and colored by functional groups.

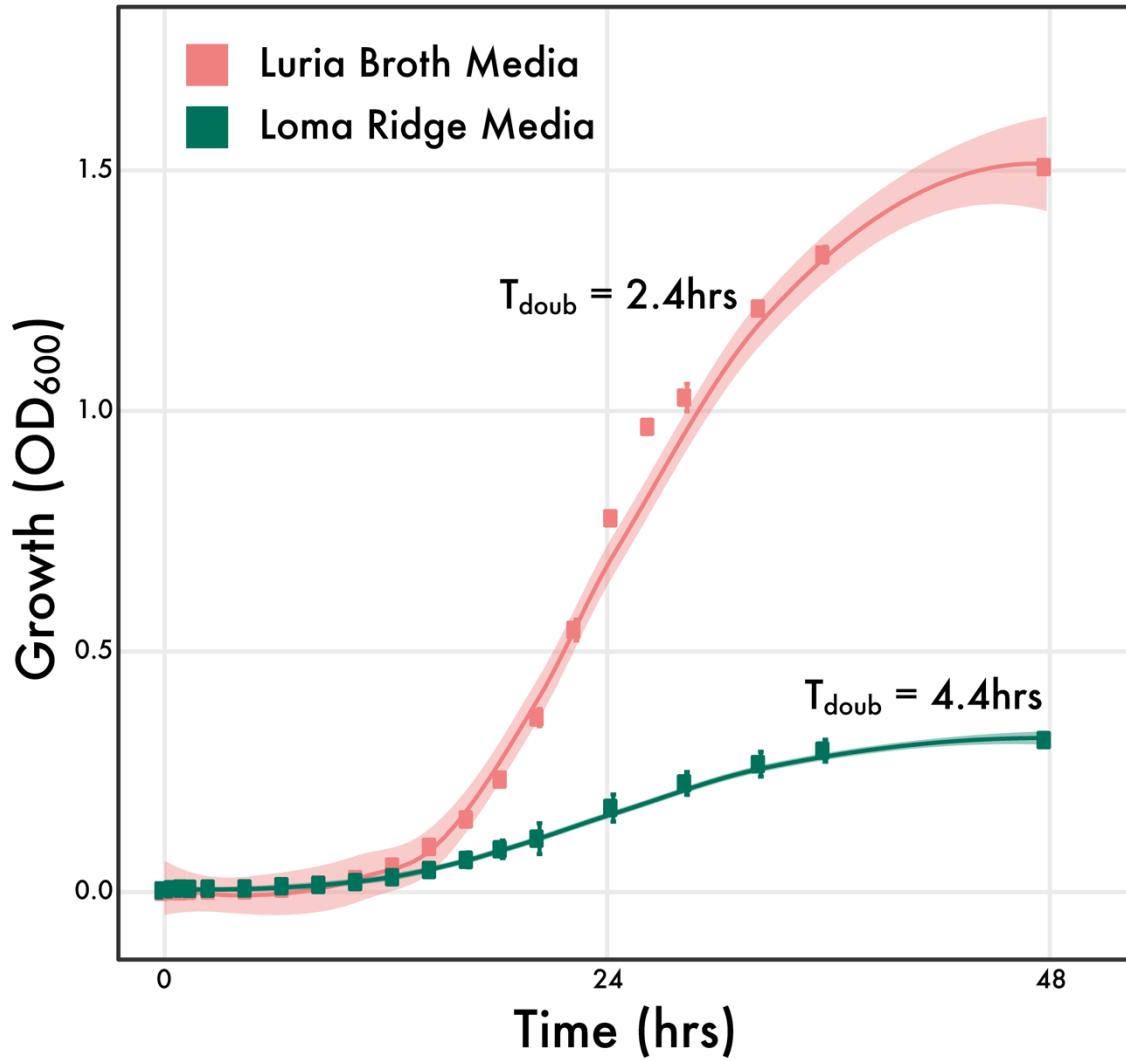


Fig. S7. Growth curves of the ancestral strain MMLR14002 across time (hrs) in high and low nutrient media (i.e., LB and LR media, respectively). Each time point plots a point for the mean (\pm 1 SD) growth. Growth curves are visualized using smoothed averages from locally weighted smoothing (LOESS) of the mean growth values. Loma Ridge (LR) media made from Grassland litter leachate.

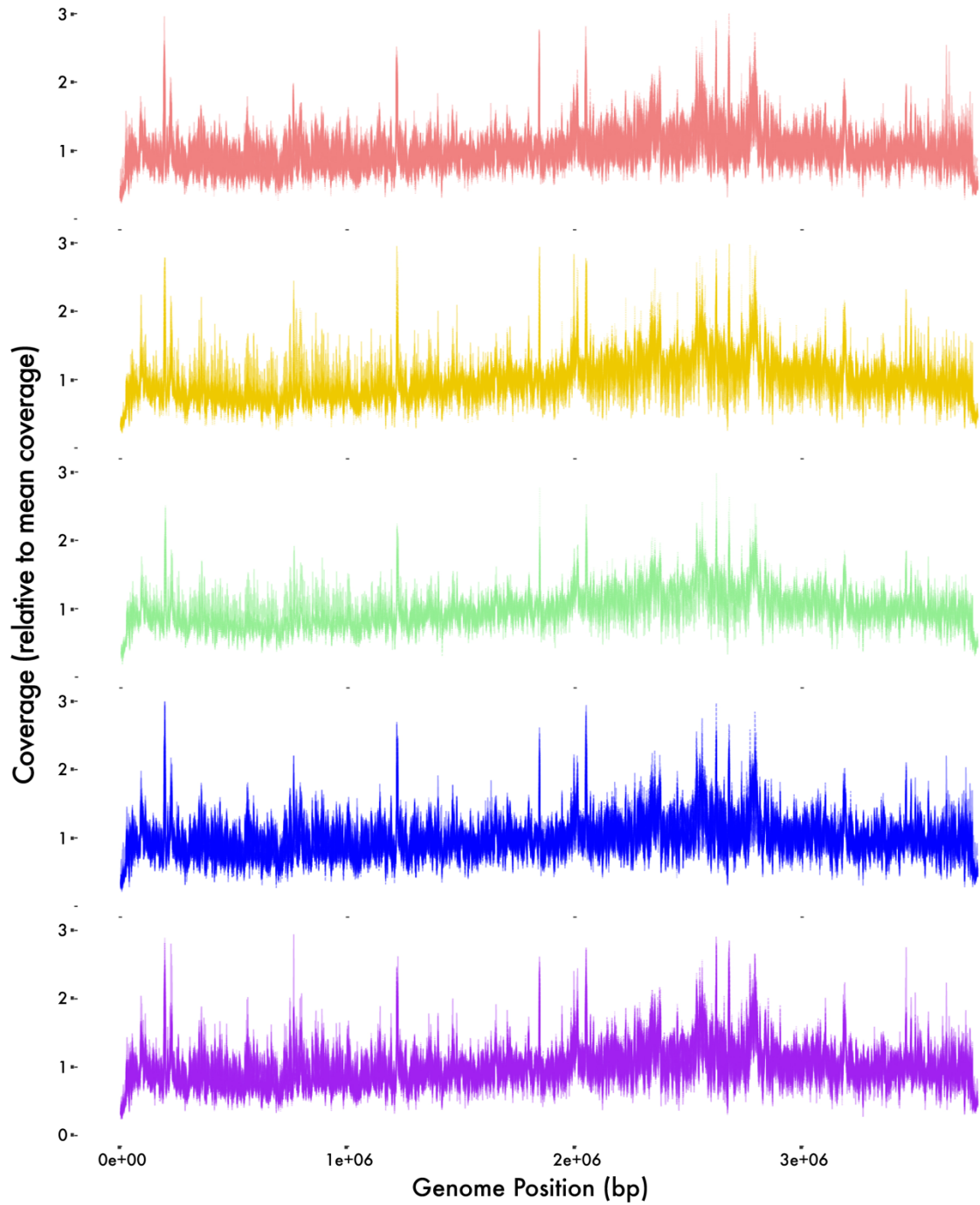


Fig. S8. Relative coverage of metagenomic samples to the reference genome across sites. Mean coverage for all sites is denoted as 1x.

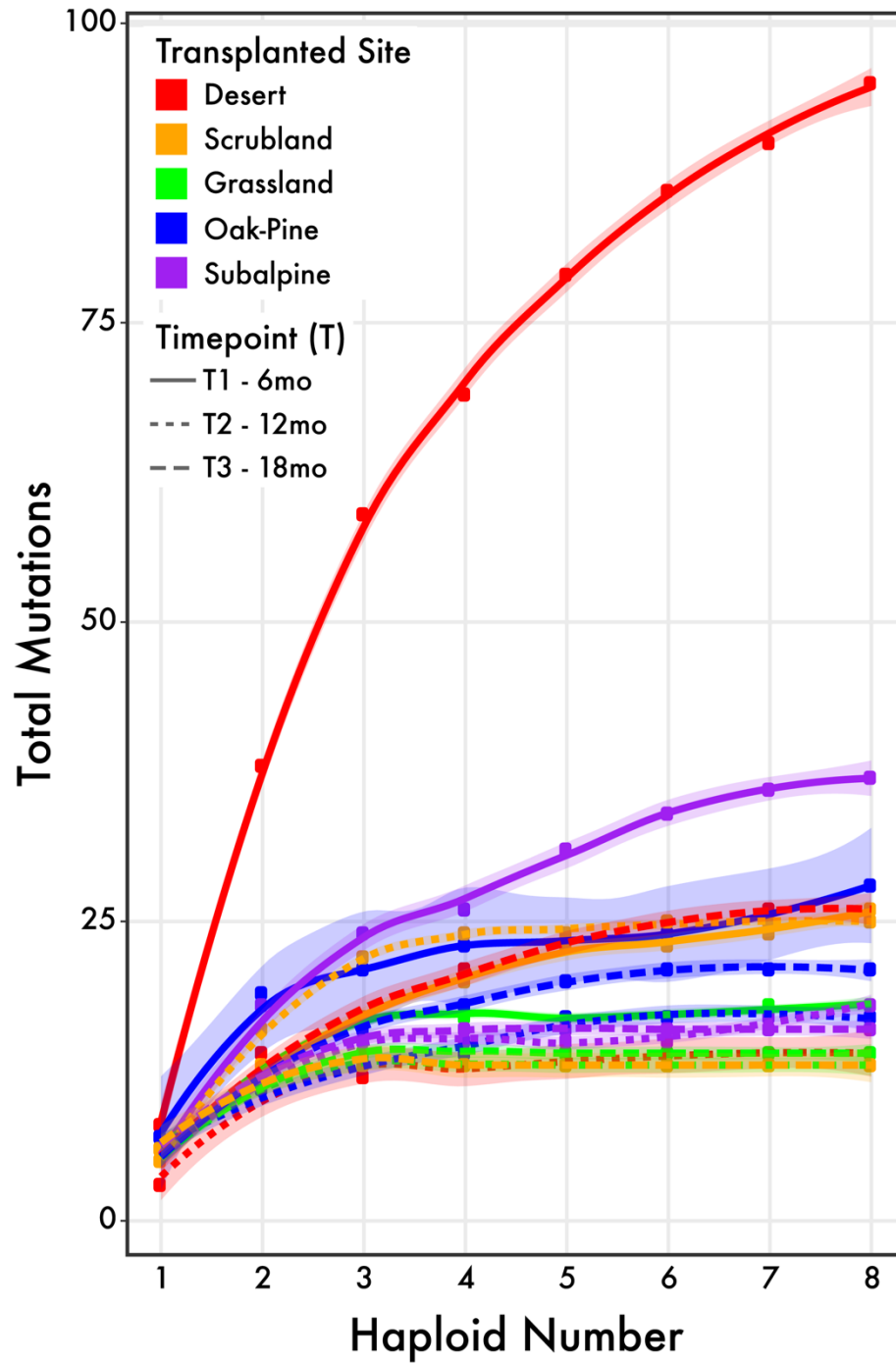


Fig. S9. Total number of variants called based on increasing haploid number in the GATK pipeline. Based on saturation for most samples and the expected strain heterogeneity in population samples, we selected H=3 for all variant calling.

SI References

1. N. R. Baker, S. D. Allison, Extracellular enzyme kinetics and thermodynamics along a climate gradient in southern California. *Soil Biol. Biochem.* 114, 82–92 (2017).